PROCEEDINGS OF SCIENCE

Probing the blue axion with Cosmic Optical Background anisotropies

Giuseppe Lucente[a,b,c,d,*]

[a] *Dipartimento Interateneo di Fisica "Michelangelo Merlin," Via Amendola 173, 70126 Bari, Italy*

[b] *Istituto Nazionale di Fisica Nucleare - Sezione di Bari, Via Orabona 4, 70126 Bari, Italy*

[c] *Institut für Theoretische Physik, Universität Heidelberg, Philosophenweg 16, 69120, Heidelberg, Germany*

[d] *Universität Heidelberg, Kirchhoff-Institut für Physik, Im Neuenheimer Feld 227, 69120 Heidelberg, Germany*

E-mail: giuseppe.lucente@ba.infn.it

A radiative decaying Big Bang relic with a mass $m_a \simeq 5 - 25$ eV, which we dub "blue axion", can be probed with direct and indirect observations of the cosmic optical background (COB). The strongest bounds on blue-axion cold dark matter come from the Hubble Space Telescope (HST) measurements of COB anisotropies at 606 nm, excluding the simple interpretation of the excess in the diffuse COB detected by Long Range Reconnaissance Imager (LORRI) as photons produced by a decaying relic. We suggest that new HST measurements at higher frequencies (336 nm and 438 nm) can improve current constraints on the lifetime up to an order of magnitude, and we show that also thermally produced and hot relic blue axions can be competitively probed by COB anisotropies.

XVIII International Conference on Topics in Astroparticle and Underground Physics (TAUP2023)
28.08-01.09.2023
University of Vienna

*Speaker

PoS(TAUP2023)036

1. Introduction

The extragalactic background light (EBL) is the integrated intensity of all the radiation emitted in the cosmic history, ranging from far-infrared to ultraviolet bands. A robust lower bound on the cosmic optical background (COB) is obtained through the Hubble Space Telescope (HST) galaxy counts [1]. However, the COB can be measured using different strategies, e.g. by directly detecting it with a spacecraft. In this context, the COB measured by the Long Range Reconnaissance Imager (LORRI) instrument on NASA's New Horizons mission is about $\sim 4\sigma$ above the HST galaxy count estimate [2], suggesting the existence of an unaccounted for EBL component, whose origin has not been explained yet. An alternative to the above mentioned approaches relies on measuring the anisotropies rather than the diffuse intensity of the COB. The LORRI excess can be interpreted as dark matter (DM) decaying to monoenergetic photons. In this context, such an excess can be produced by DM axion-like particles a with mass $m_a \simeq 5 - 25\,\mathrm{eV}$ decaying to blue and ultraviolet light, hereafter dubbed "blue axions" [3]. In this contribution we will show that HST anisotropy measurements at 606 nm exclude the hypothesis that the excess is due to decaying DM blue axions, for both the cold dark matter (CDM) and non-cold dark matter (NCDM) scenarios, and that new dedicated HST measurements at 336 nm and 438 nm can set stronger constraints on the lifetime of the blue axion, resulting in the best probe to date. This work is based on the results obtained in Ref. [4], to which we address the interested reader for further details.

2. Isotropic and anisotropic cosmic optical background

We consider a population of blue axions interacting with photons through the Lagrangian

$$\mathcal{L} \supset \frac{1}{4} g_{a\gamma\gamma} a F_{\mu\nu} \tilde{F}^{\mu\nu}, \tag{1}$$

where $F_{\mu\nu} = \partial_\mu A_\nu - \partial_\nu A_\mu$, $\tilde{F}_{\mu\nu} = \epsilon_{\rho\sigma\mu\nu} F^{\rho\sigma}/2$ and $g_{a\gamma}$ is the axion-photon coupling. This interaction allows blue axions to decay to two photons with a rate $\Gamma_{a\to\gamma\gamma} = g_{a\gamma\gamma}^2/64\pi\, m_a^3$, contributing to the COB. Assuming the relic decays at rest, the decay spectrum of photons is monochromatic with energy $\omega_{\max} = m_a/2$ and the energy gets redshifted. Thus, the intensity can be written as $\langle I(\omega)\rangle = \frac{\omega}{4\pi}\frac{\rho_a}{m_a}\frac{2\,\Gamma_{a\to\gamma\gamma}}{H(\tilde{z})}$ [5], where $\tilde{z} = \omega_{\max}/\omega - 1$ and $H(z)$ is the Hubble parameter at the redshift z. In this context, the excess detected by LORRI can be explained assuming blue axions to constitute 100% of the dark matter with a decay rate $\Gamma_{a\to\gamma\gamma} \simeq 10^{-23} - 10^{-22}\,\mathrm{s}^{-1}$.

Since blue axions can be clumped, their decay can show up anisotropically in the sky. In this context, the relevant angular power spectrum can be written as

$$C_l(\omega_{\rm piv}) = \int_0^\infty dz \left[\frac{1}{4\pi}\frac{\omega_{\rm piv}^2}{\omega_{\max} H(z)}\frac{\rho_a}{m_a} 2\Gamma_{a\to\gamma\gamma}\right]^2 \left[\epsilon\left(\frac{\omega_{\max}}{1+z}\right)\right]^2 \frac{H(z)}{r(z)^2} P_\delta\left[k = \frac{l}{r(z)}, r(z), r(z)\right], \tag{2}$$

where $\omega_{\rm piv}$ and $\epsilon(\omega)$ are the pivot wavelength and the normalized throughput function of the detector, i.e. the Wide Field Camera 3 on board of the Hubble Space Telescope,[1] while the abundance ρ_a and the non-linear spatial power spectrum P_δ depend on the production mechanism.

[1] https://www.stsci.edu/hst/instrumentation/wfc3

3. Production mechanisms

We first assume that blue axions in the mass range $5 - 25\,\mathrm{eV}$ constitute 100% of dark matter. In this context, since the QCD axion in the $5 - 25\,\mathrm{eV}$ mass range is largely excluded by several bounds, one can consider generic axion-like particles, produced via misalignment mechanism and topological defect decay [6]. These mechanisms would produce CDM blue axions, with abundance $\rho_a = \rho_{\rm CDM} = \Omega_{\rm CDM}\rho_c$, where $\Omega_{\rm CDM} = 0.12\,h^{-2}$ and $\rho_c = 1.05 \times 10^{-5} h^2\,\mathrm{GeV\,cm^{-3}}$, with $h = 0.674$, and the non-linear power spectrum $P_\delta(z, r, r)$ evaluated with the CLASS code [7], publicly available.[2]

Axions interacting with photons can be produced in the early Universe plasma via Primakoff effect $\gamma Q \to aQ$, where Q refers to any charged particle, and behave as a NCDM component. Axions decouple from the thermal plasma at a freeze-out temperature T_F at which their interaction rate with the SM particles becomes lower than the expansion rate. For the Primakoff process, $T_F \simeq 4 \times 10^4 \mathrm{GeV} \left(\frac{g_{a\gamma\gamma}}{10^{-11}\ \mathrm{GeV}^{-1}}\right)^{-2}$ [8], implying that for $g_{a\gamma\gamma} \lesssim 10^{-9}\ \mathrm{GeV}^{-1}$, T_F is larger than the Electroweak (EW) scale. After decoupling, the axion population established at the freeze-out temperature redshifts until today, with abundance and temperature T_a given by [8]

$$\Omega_a h^2 = \frac{m_a}{13\ \mathrm{eV}} \frac{1}{g_{*,s}(T_F)}, \qquad \frac{T_a}{T_0} = \left(\frac{g_{*,s}(T_0)}{g_{*,s}(T_F)}\right)^{1/3}, \tag{3}$$

where $g_{*,s}(T)$ is the number of entropy-degrees of freedom and $T_0 = 0.235$ meV is the Cosmic Microwave Background temperature, at which $g_{*,s}(T_0) = 3.91$. The NCDM abundance is constrained to be much smaller than the CDM one by structure formation observations, as shown in Ref. [9] assuming a NCDM component with temperature equal to standard neutrinos $T_{\rm NCDM} = T_\nu = 0.716\,T_0$. Since cosmological calculations depend on the ratio $m_{\rm NCDM}/T_{\rm NCDM}$, the bound on the NCDM abundance in Ref. [9] can be translated for a NCDM axion with mass m_a and temperature T_a rescaling the mass accordingly, i.e. $m_a/T_a = m_{\rm NCDM}/T_\nu$. For $m_a \sim \mathcal{O}(10)$ eV, the axion relic abundance is much larger than the structure formation constraints, ruling out the freeze-out mechanism in the context of the SM. Thus, we consider NCDM axions produced in two alternative scenarios.

- *A modified freeze-out scenario*, in which axions decouple at a temperature larger than the EW scale, where the particle content of the plasma is speculative. Thus, we assume additional degrees of freedom to increase $g_{*,s}$, reducing the axion relic abundance and temperature to satisfy the structure formation bound. For each value of m_a, we evaluate the angular power spectrum using ρ_a obtained from Eq. (3) and the non-linear NCDM power spectrum computed in the adiabatic approximation $P_{\delta,\rm NCDM} = (\mathcal{T}_{\rm NCDM}/\mathcal{T}_{\rm CDM})^2\, P_{\delta,\rm CDM}$, where $\mathcal{T}_{\rm NCDM}$ and $\mathcal{T}_{\rm CDM}$ are the transfer functions of NCDM and CDM [10]. We obtain both the transfer functions and the non-linear CDM power spectrum $P_{\delta,\,\rm CDM}$ using CLASS, with parameters m_a, Ω_a and T_a from Eq. (3), computed using the value of $g_{*,s}$ satisfying the structure formation bound.

- *A hot relic scenario*, in which relic axions have the neutrino temperature T_ν and their abundance saturates the bounds in Ref. [9]. In this scenario, we compute the angular power spectrum C_l in Eq. (2) with the axion relic density saturating the structure formation constraint in

[2] https://lesgourg.github.io/class_public/class.html

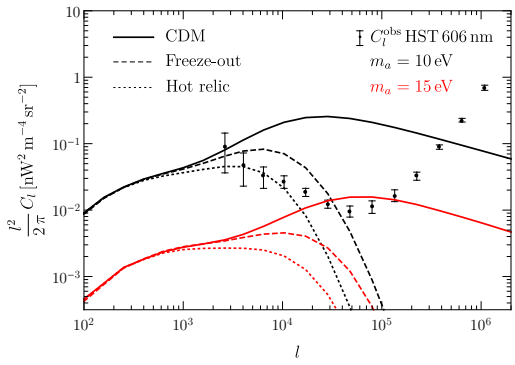

Figure 1: Angular power spectrum for decaying DM axions, observed at 606 nm, in the CDM (solid lines), freeze-out (dashed) and hot relic (dotted) scenarios for $m_a = 10$ eV (black lines) and $m_a = 15$ eV (red). We have fixed $\rho_a\,\Gamma_{a\to\gamma\gamma} = 10^{-29}\,\mathrm{s}^{-1}\,\mathrm{GeV\,cm}^{-3}$. The HST measurements are shown with error bars [11].

Ref. [9] [without satisfying Eq. (3)] and the non-linear NCDM power spectrum computed in the adiabatic approximation, obtaining $\mathcal{T}_{\rm NCDM}$, $\mathcal{T}_{\rm CDM}$ and $P_{\delta,\rm CDM}$ through CLASS using as input parameters m_a, $T_a = T_\nu = 0.716\,T_0$ and Ω_a from Ref. [9].

4. Results

The resulting angular power spectra in the different scenarios previously discussed can be compared with the HST measurements at the shortest available wavelength, namely 606 nm [11]. In Fig. 1 we show the angular power spectrum $l^2\,C_l/2\pi$ as measured by HST at 606 nm with error bars, and the angular power spectrum from decaying DM as seen by the detector at 606 nm, at fixed value of $\rho_a\,\Gamma_{a\to\gamma\gamma} = 10^{-29}\,\mathrm{s}^{-1}\,\mathrm{GeV\,cm}^{-3}$ for $m_a = 10$ eV (black lines) and $m_a = 15$ eV (red lines). We constrain the blue axion lifetime by requiring that the angular power spectrum C_l in Eq. (2) does not exceed the upper error bar of any data point.

In the case of CDM (solid lines) the quantity $l^2\,C_l$ is peaked at $l \gtrsim 10^4$ and the peak is shifted towards smaller scales as the mass increases. In this context, we exclude the light blue region delimited by the solid line in the upper panel of Fig. 2. Stronger constraints on the axion lifetime could be obtained with HST measurements at shorter wavelengths. In order to forecast the possible future reaches, we evaluate the angular power spectrum in Eq. (2) using $\omega_{\rm piv}$ and $\epsilon(\omega)$ for measurements at 438 nm and 336 nm, respectively, and we require that it does not exceed the upper error bar of any data point at 606 nm. In this way we probe the light blue regions delimited by dashed lines in Fig. 2 (upper panel), labelled with HST 438 nm and HST 336 nm, respectively. Measurements at 336 nm would improve the current anisotropy bound by a factor 4-10 in the mass range $10 - 25$ eV, leading to the strongest constraints in this region.

The anisotropy bounds can be relaxed for NCDM axions since the resulting angular power spectrum C_l can be smaller due to a lower relic abundance ρ_a and the suppression of the non-linear power spectrum P_δ. In Fig. 1 we show the resulting angular power spectrum for the cases of freeze-out (dashed) and of a hot relic with neutrino temperature (dotted). The effect of the abundance suppression is blurred out since the angular power spectra are shown at fixed value of $\rho_a\Gamma_{a\to\gamma\gamma}$.

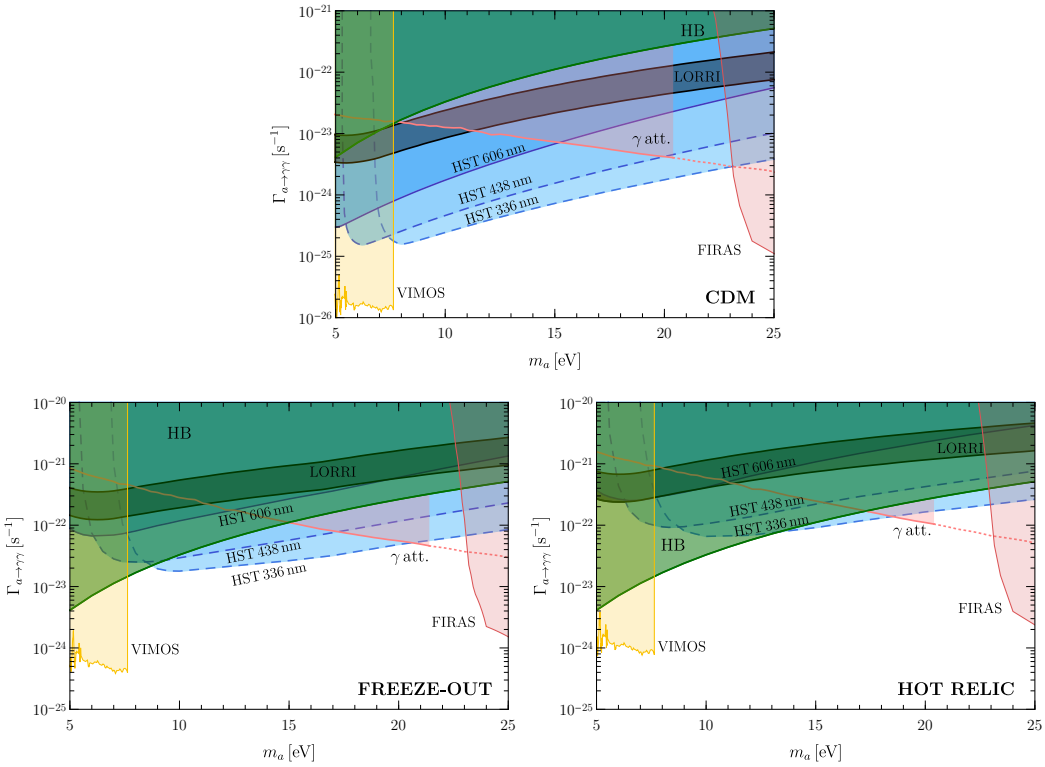

Figure 2: Bounds and projected reaches on the blue axion lifetime in the case of CDM (upper panel), freeze-out (lower left) and hot relic (lower right). The 606 nm bound is the solid blue line, while the forecasts of our proposed observations at 438 nm and 336 nm are the dashed blue lines. The black band identifies the 95% CL excess detected by LORRI [2, 3]. For details on other bounds see Ref. [4] and references therein.

On the other hand, the effect of the non-linear power spectrum suppression is clearly visible, since for NCDM the quantity $l^2\, C_l$ is suppressed at $l \lesssim 10^4$. The suppression point is at larger scales for hotter DM and, for a fixed cosmological scenario, the suppression starts at smaller scales as the mass increases, reflecting the trend of the non-linear power spectrum. In Fig. 2 we show how the bounds on the axion lifetime are relaxed in the freeze-out (lower left panel) and hot relic (lower right panel) scenarios. In these cases, future measurements at shorter wavelengths would improve the current anisotropy bound by almost one order of magnitude, setting the strongest probe on the blue axion lifetime for 10 eV $\lesssim m_a \lesssim$ 20 eV (freeze-out) and 15 eV $\lesssim m_a \lesssim$ 18 eV (hot relic).

5. Conclusions

In this work, I have revisited the parameter space of a radiative decaying Big Bang relic with a mass $m_a \simeq 5 - 25$ eV, dubbed "blue axion", considering three different scenarios, namely cold dark matter produced through the misalignment mechanism (with additional contributions from topological defects), a thermally produced population with temperature set by a freeze-out mechanism, and a hot relic with the temperature of neutrinos and the maximum abundance allowed by structure formation bounds. In this mass range, cosmic optical background anisotropies are a powerful probe of DM axions. Indeed, current measurements of the COB anisotropies with HST

at the pivot wavelength of 606 nm exclude the interpretation of the LORRI excess as decaying DM axions and future observations at shorter wavelengths (438 nm and 336 nm) will give the possibility to explore currently unprobed regions of the axion parameter space.

Acknowledgments

GL is supported by the European Union's Horizon 2020 Europe research and innovation programme under the Marie Skłodowska-Curie grant agreement No 860881-HIDDeN.

References

[1] S. P. Driver, S. K. Andrews, L. J. Davies, A. S. G. Robotham, A. H. Wright, R. A. Windhorst, S. Cohen, K. Emig, R. A. Jansen and L. Dunne, "Measurements of Extragalactic Background Light From the far UV to the far IR From Deep Ground- and Space-based Galaxy Counts," Astrophys. J. **827** (2016) no.2, 108 doi:10.3847/0004-637X/827/2/108 [arXiv:1605.01523 [astro-ph.GA]].

[2] T. R. Lauer, M. Postman, J. R. Spencer, H. A. Weaver, S. A. Stern, G. R. Gladstone, R. P. Binzel, D. T. Britt, M. W. Buie and B. J. Buratti, *et al.* "Anomalous Flux in the Cosmic Optical Background Detected with New Horizons Observations," Astrophys. J. Lett. **927** (2022) no.1, L8 doi:10.3847/2041-8213/ac573d [arXiv:2202.04273 [astro-ph.GA]].

[3] J. L. Bernal, G. Sato-Polito and M. Kamionkowski, "Cosmic Optical Background Excess, Dark Matter, and Line-Intensity Mapping," Phys. Rev. Lett. **129** (2022) no.23, 231301 doi:10.1103/PhysRevLett.129.231301 [arXiv:2203.11236 [astro-ph.CO]].

[4] P. Carenza, G. Lucente and E. Vitagliano, "Probing the blue axion with cosmic optical background anisotropies," Phys. Rev. D **107** (2023) no.8, 083032 doi:10.1103/PhysRevD.107.083032 [arXiv:2301.06560 [hep-ph]].

[5] O. E. Kalashev, A. Kusenko and E. Vitagliano, "Cosmic infrared background excess from axionlike particles and implications for multimessenger observations of blazars," Phys. Rev. D **99** (2019) no.2, 023002 doi:10.1103/PhysRevD.99.023002 [arXiv:1808.05613 [hep-ph]].

[6] C. A. J. O'Hare, G. Pierobon, J. Redondo and Y. Y. Y. Wong, "Simulations of axion-like particles in the postinflationary scenario," Phys. Rev. D **105** (2022) no.5, 055025 doi:10.1103/PhysRevD.105.055025 [arXiv:2112.05117 [hep-ph]].

[7] D. Blas, J. Lesgourgues and T. Tram, "The Cosmic Linear Anisotropy Solving System (CLASS) II: Approximation schemes," JCAP **07** (2011), 034 doi:10.1088/1475-7516/2011/07/034 [arXiv:1104.2933 [astro-ph.CO]].

[8] D. Cadamuro, "Cosmological limits on axions and axion-like particles," [arXiv:1210.3196 [hep-ph]].

[9] R. Diamanti, S. Ando, S. Gariazzo, O. Mena and C. Weniger, "Cold dark matter plus not-so-clumpy dark relics," JCAP **06** (2017), 008 doi:10.1088/1475-7516/2017/06/008 [arXiv:1701.03128 [astro-ph.CO]].

[10] D. Inman and U. L. Pen, "Cosmic neutrinos: A dispersive and nonlinear fluid," Phys. Rev. D **95** (2017) no.6, 063535 doi:10.1103/PhysRevD.95.063535 [arXiv:1609.09469 [astro-ph.CO]].

[11] K. Mitchell-Wynne, A. Cooray, Y. Gong, M. Ashby, T. Dolch, H. Ferguson, S. Finkelstein, N. Grogin, D. Kocevski and A. Koekemoer, *et al.* "Ultraviolet Luminosity Density of the Universe During the Epoch of Reionization," Nature Commun. **6** (2015), 7945 doi:10.1038/NCOMMS8945 [arXiv:1509.02935 [astro-ph.CO]].